ARKIV FÖR FYSIK Band 13 nr 37

Communicated 12 February 1958 by Manne Siegbahn and Erik Rudberg

Evidence of chemical shifts of the inner electronic levels in a metal relative to its oxides (Cu, Cu_2O, CuO)

By Carl Nordling, Evelyn Sokolowski and Kai Siegbahn

With 10 figures in the text

ABSTRACT

The energies of some inner electronic levels of copper have been studied in the case of the pure metal and the cuprous and cupric oxides by means of magnetic analysis of X-ray produced photo electrons. In all cases a shift has been observed towards greater binding energy on going from the metal to the oxide, this shift being greatest (4.4 eV) for the $1s$ and $2s$ levels in the cupric oxide. The observed shift in K binding energy for CuO can be correlated to the results of entirely different investigations on the band structure of the oxide. Indications have been found of changes in the natural line widths in connection with oxidation.

A line in the KLL Auger spectrum from metallic copper has been compared with the corresponding line from CuO. The line from the oxide has been found to be somewhat lower in energy. Also, there is some evidence that the K Auger yield depends on the chemical composition of the source.

I. Introduction

A method has previously been described for the study of electronic binding energies in metals [1]. The basis of the method was the magnetic analysis of photo electrons, expelled from thin, evaporated metal layers by X-radiation. Since the accuracy in such investigations can be brought up to a few tenths of an electron volt even for heavy elements, it has been natural to extend the method to investigations of changes in the electronic binding energies of a metal in connection with compound- or alloy formation. The K and L levels of Cu have been studied in the present investigation, both in the pure metal and in the $+1$ and $+2$ states of oxidation. In connection with chemical shifts of electronic energy levels the total binding energy (where the work function is included) is slightly ambiguous, since the work function may vary on account of surface changes that, from a theoretical point of view, are uninteresting. By putting a reference potential just outside the source, the effect of the work function was eliminated, and all the inner electronic levels could be referred to the Fermi level of the source (see section V A).

II. Apparatus

The apparatus consists of an X-ray tube together with an iron-free double-focussing β-spectrometer. The X-radiation produces photo electrons in a converter of the material under investigation, which are then analyzed magnetically with the spectrometer. A detailed description of the general features of the set-up has already been given in reference [1].

In determining the energy shift of a photo line as it originates in converters of different chemical composition, it is essential to make the measurements without changing the geometry of the source. In order to make this possible the source holder was redesigned as illustrated in Fig. 2. The converter frame was made in three sections, which could be exposed to the X-ray beam successively by sliding the frame up or down. The frame was constrained to move only in the vertical direction. The sample backing, a single aluminum strip with a thickness of 25 μ and a width of approximately 1 mm, was stretched across all three sections of the frame and fastened at the ends with brass plates. The converter material was deposited on the aluminum backing so that the middle section held the compound under investigation (copper oxide) and the two outer sections the reference material (metallic copper), or vice

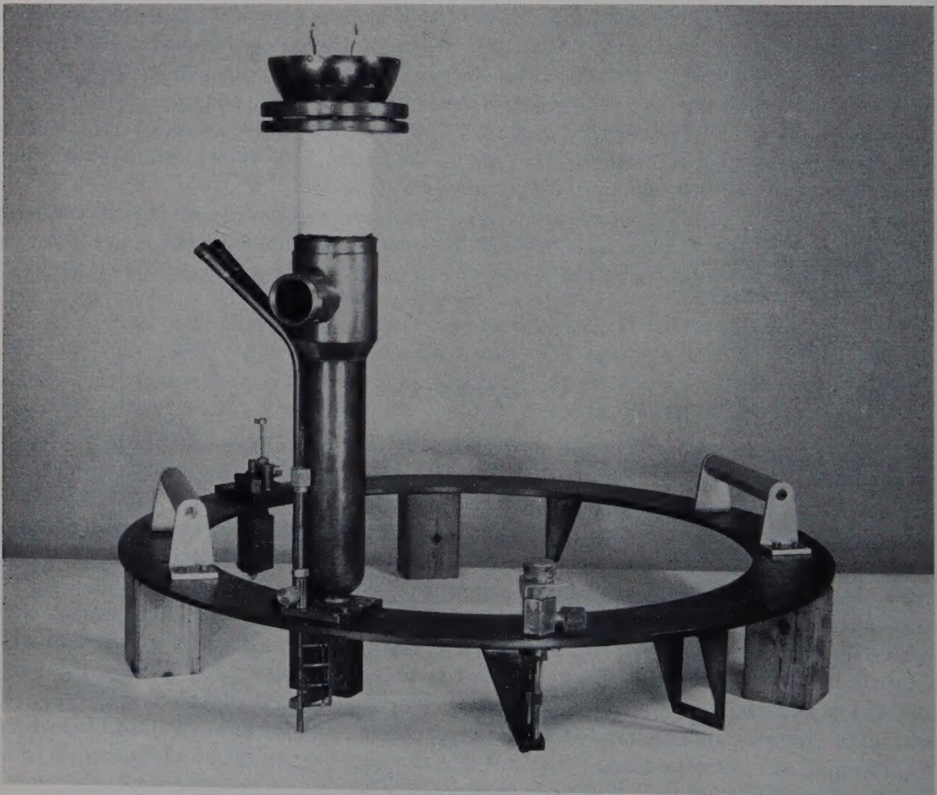

Fig. 1. Lid of spectrometer tank, with X-ray tube, source holder, G.M. detector and baffles.

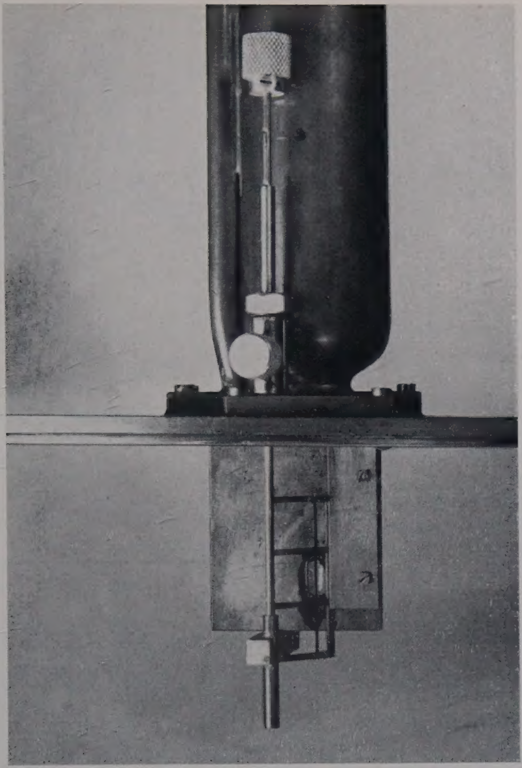

Fig. 2. Lower part of X-ray tube, together with the electron source. The X-radiation passes through a 20 μ aluminum window and strikes the converter at a 45° angle, the 90° angle of optimum photo electron yield being along the spectrometer axis. The three sections of the converter can be exposed to the X-ray beam successively by sliding the frame up or down. The electrode defining the reference potential has been removed for clarity.

versa. In this way the lines from the outer sections gave a check on the reproducibility of the source position. When the converter material was evaporated onto the backing, the latter was always covered with a straight mask, having a slit 0.6 mm wide, and extending across all three sections of the backing.

The oxide was prepared by first making an ordinary vacuum deposit of metallic copper, about 100 Å thick, on the appropriate section of the backing, which was then exposed to oxygen under varying conditions (see section III). When the oxidation was completed, metallic copper was evaporated onto the remaining sections of the backing, after which the sample was transferred to the vacuum tank of the spectrometer within a few minutes. During the whole evaporation and oxidation process the mask was retained in front of the backing, so that the three samples lay on a straight line. If a shift was observed between the photo lines from the two identical outer samples, the proper position of the corresponding line from the middle section could be inferred by means of linear interpolation. It was usually possible to adjust the converter deposit visually with the aid of a telescope to be parallel to the edge of the frame. This is illustrated in Fig. 3, which shows K photo lines from the three sections

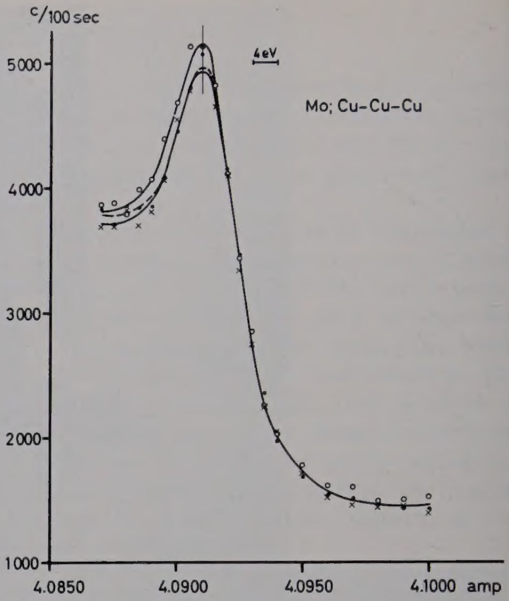

Fig. 3. *K* photo lines from the three sections of the source holder, with metallic copper on all three sections. The figure illustrates a case where the orientation of the source was perfectly parallel to the edge of the frame.

of the source holder, with metallic Cu on all three sections. All three lines coincide, which proves that there has been no change in geometry. To justify the linear interpolation in the cases where there was a slight shift between the lines from the outer sections, the source backing and mask were purposely mounted at an angle of 1°.5 with the edge of the frame. With the same converter material on all three sections, the three photo lines were equidistant, the shift between the two outer lines being 0.19 gauss-cm.

The possibility of a change in work function on going from the metal to the oxide must be taken into account. Since such a change was of little interest in the present case, its effect was eliminated by making the electrons pass a defined potential surface before the magnetic analysis. The defining electrode was in the form of a fine metal mesh (hole diameter 0.05 mm, transmission 80 %), made of the same material as and grounded to the spectrometer tank, thus representing the vacuum potential of the spectrometer. Care was taken that the electrode did not interfere with the X-ray beam. The performance of the electrode was tested by charging up the source to a known voltage (4 V) with respect to the spectrometer. It was found that the potential change was well reproduced in the line shift. As shown below (section VA), the energy shift with respect to the spectrometer vacuum level is equivalent to a shift with respect to the Fermi level of the material under investigation.

Since the expected energy shifts were at most of the order of a few electron volts, it was essential to keep the different spectrometer parameters under rigorous control. If, for instance, a temperature gradient arises in the spectrometer, this will cause an apparent line shift according to equation 5, reference [2]. Thus, if the temperature of the tank rises 1°C with respect to the two coils, the resulting relative momentum shift will be $8:10^6$. In order to avoid temperature variations, the spectrometer was equipped with a temperature control system, consisting of copper-constantan thermocouples, placed at several points in the spectrometer tank as well as in the

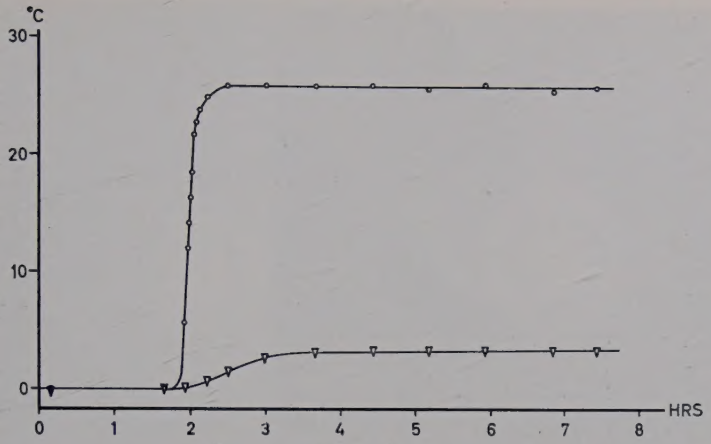

Fig. 4. Temperature of the spectrometer tank relative to that of the inner bobbin as a function of time. The upper curve corresponds to a point in the tank close to the X-ray tube, the lower to a point near the detector. The sudden rise in temperature corresponds to the switching on of the X-ray tube. It is seen that after the tube has been turned on, equilibrium is reached within two hours.

bobbins of the coils. The thermocouple junctions were soldered into metal caps, which fitted into cavities in the spectrometer. The greatest temperature change occurred in the spectrometer tank on switching on the X-ray tube, which, at normal operation, develops a power of 1 kW. Fig. 4 shows the temperature change of two points in the spectrometer tank with respect to the inner bobbin. The upper curve corresponds to a point near the X-ray tube, and the lower to one near the detector. It is seen that equilibrium is reached within about $1\frac{1}{2}$ hours.

A disturbing factor in the measurements were stray magnetic fields from various other laboratories that had to be compensated with the Helmholtz field.

III. Preparation of sources

Three methods were used for the oxidation of the films. One method was to simply heat the film in air at about 225°C for at least 15 hours. Alternatively, the oxidation was accomplished in an oxygen atmosphere containing some 8 % ozone. In the latter case the temperature was kept at 125°C and the process allowed to go on for 20 minutes. Films oxidized in these different ways gave the same energy shift of the *K* photo lines within experimental error. Under the above conditions CuO is believed to be formed. As the thickness of the copper films is only of the order of 100 Å, the solid phase reaction giving Cu_2O is assumed to be negligible in this case [3]. This was checked by taking electron diffraction patterns of the samples (see below). Another possible process is the diffusion of copper atoms into the lattice of the aluminum backing during the heating of the sample, resulting in a Cu-Al alloy which might give a shift of the binding energies. That this effect was small was shown by heating one sample in a hydrogen atmosphere, which prevented oxidation. The temperature and time of reaction were the same as for oxidation to CuO in air. A measurement on this sample gave an upper limit for the *K* level shift of 1 eV.

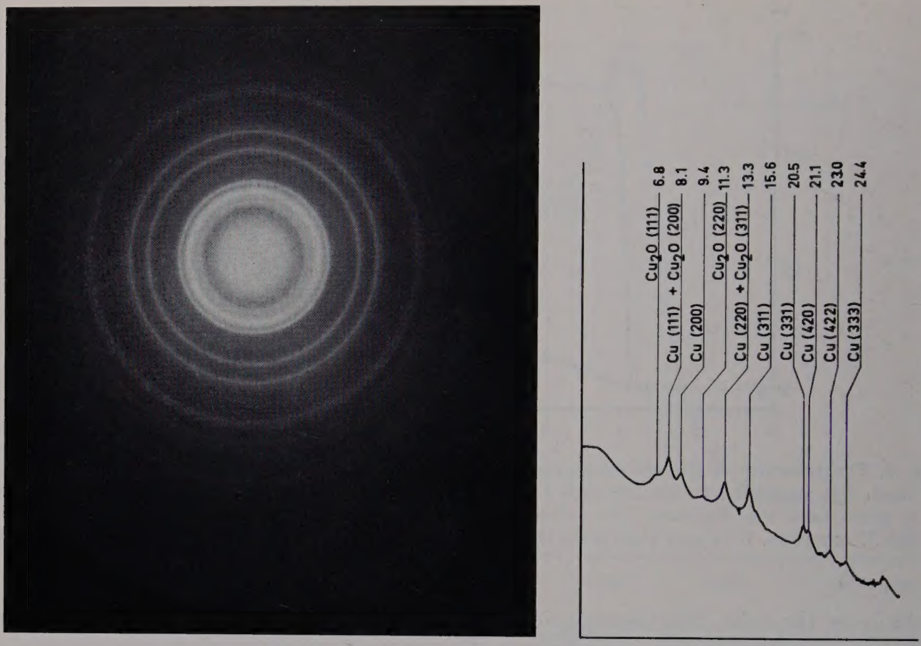
Cu_2O (111) 6.8
Cu (111) + Cu_2O (200) 8.1
Cu (200) 9.4
Cu_2O (220) 11.3
Cu (220) + Cu_2O (311) 13.3
Cu (311) 15.6
Cu (331) 20.5
Cu (420) 21.1
Cu (422) 230
Cu (333) 24.4

Fig. 5*a*

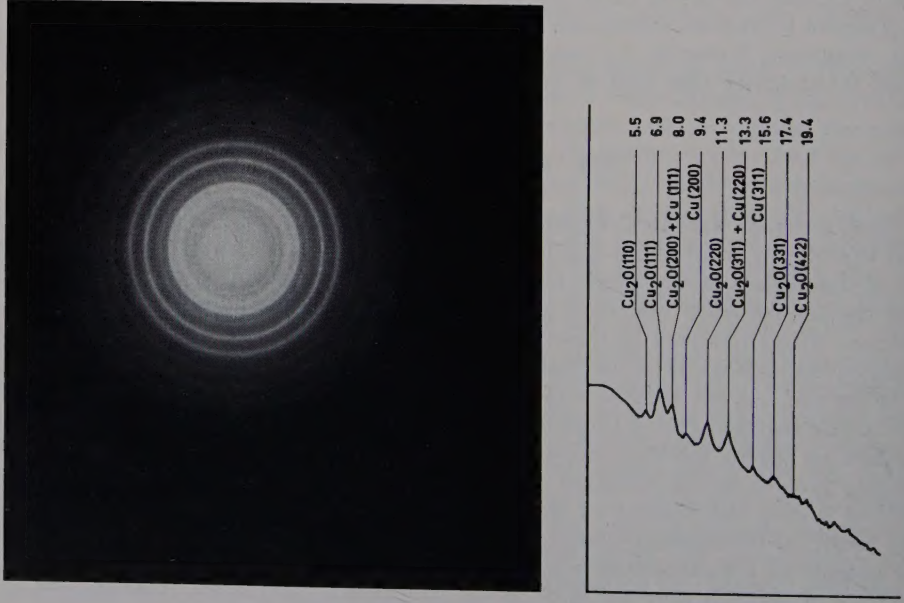
Cu_2O(110) 5.5
Cu_2O(111) 6.9
Cu_2O(200) + Cu (111) 8.0
Cu(200) 9.4
Cu_2O(220) 11.3
Cu_2O(311) + Cu(220) 13.3
Cu(311) 15.6
Cu_2O(331) 17.4
Cu_2O(422) 19.4

Fig. 5*b*

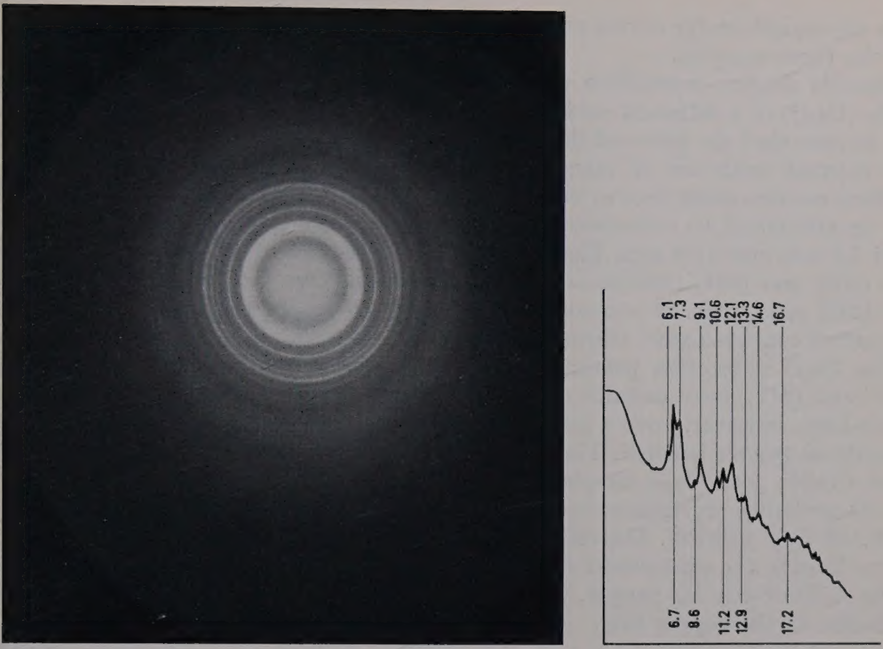

Fig. 5*c*

Fig. 5. Electron diffraction patterns of the three different types of samples, and photometer curves of the ring intensities. The ring radii (in mm) and reflecting plane indices are also given. Fig. *a* is for metallic copper, *b* for Cu_2O, and *c* for CuO.

If the temperature and time of oxidation are considerably decreased, the main oxide formed is Cu_2O [4]. In order to study the shift in Cu_2O the time of oxidation (in air) was reduced to 1 hour and the temperature to 125°C.

It is a well-known fact that there is a certain amount of oxidation even at room temperature [5, 6]. A Cu_2O film of at most about 25 Å is formed after a few hours exposure to air of atmospheric pressure and room temperature, the first ten or fifteen Ångströms forming very rapidly within a few minutes. To minimize the oxidation of the "pure" copper converters, these were always put into the spectrometer as soon as possible after the evaporation, after which the apparatus was evacuated. Nevertheless it is clear that the exposure to oxygen before the film was examined was sufficient for the first 10 Å or so of oxide to form. This did not, however, cause any serious difficulties as the total thickness of the copper layers was more than ten times greater.

In order to check the composition of the samples, electron diffraction patterns were taken of the pure metal and its oxides, the samples being prepared in the same way as those used in the chemical shift measurements except for the mounting. Instead of evaporating the metal onto an aluminum strip, a formvar film was used as a backing. After the evaporation the formvar was dissolved in a chloroform–alcohol mixture. The metallic film was mounted directly on a copper mesh with a transmission of about 80 %. Fig. 5 shows the three diffraction patterns obtained, together with microphotometer curves of the patterns. The accelerating voltage was the same for the three samples.

Metallic copper crystallizes in a fcc system with $a = 3.608$ Å and the cuprous oxide (Cu_2O) in a different cubic structure with $a = 4.268$ Å. From Figs 5*a* and *b* it can be seen that the ratios of the ring radii for the same reflection in metallic copper and cuprous oxide are all equal to the inverse ratio of the cell constants.

There are two weak lines in the photometer curve of the Cu pattern, Fig. 5*a*, which can be attributed to reflections in the Cu_2O structure only, namely the lines with radii 6.8 mm and 11.3 mm. These are the strong (111) and (220) reflections in Cu_2O. The (200) and (311) reflections in Cu_2O cannot be resolved from the copper (111) and (220) reflections. It is obvious that the "pure" copper sample contains a small amount of cuprous oxide, which is to be expected according to the above discussion.

The Cu_2O diffraction pattern in Fig. 5*b* contains two well resolved reflections ((200) and (311)) from metallic copper with raddii 9.4 mm and 15.6 mm respectively. These lines, however, have a low intensity in this pattern, and hence the amount of unoxidized copper is small. The process used for the oxidation of Cu to Cu_2O thus gives a fairly good Cu_2O sample.

CuO probably crystallizes in a monoclinic system with $a = 4.653$ Å, $b = 3.410$ Å, $c = 5.108$ Å, $\beta = 99°29'$. The diffraction pattern obtained is shown in Fig. 5*c*.[1] There are no lines in the photometer curve that must be attributed to reflections from cuprous oxide or metallic copper, which indicates that in this case there was a complete oxidation of the copper film.

IV. Experimental results

As shown in reference [1], each electron line consists of a peak due to unscattered electrons, together with a smaller peak at lower energy, due to electrons that have suffered a discrete energy loss upon scattering in the source. The separation of the peaks, which is characteristic of the scatterer, has been found to be about 16 eV in copper and its oxides. For the energy determinations, the "undisturbed" electron peak has been taken to represent the position of the lines.

As motivated in section V A, we have in this investigation taken the binding energy of an inner atomic level to mean the energy with respect to the Fermi level.

A. *Cu—CuO*

(i) *Binding energy shifts*

K shift.—For the investigation of the *K* binding energies, Mo $K\alpha_1$ radiation was used for the production of photo electrons. Fourteen measurements were made of the difference between the copper *K* binding energy in the pure metal and in the cupric oxide. A typical result is shown in Fig. 6. In this case the oxide layer was deposited on the middle section of the backing, with the metallic copper on each side. The peak of the oxide photo line falls at a lower energy than the lines from the

---

[1] The CuO reflections were identified by comparing the pattern with an X-ray diffraction diagram provided by Fil. lic. H. Fischmeister, Institute of Inorganic Chemistry, Uppsala, whose cooperation we wish to acknowledge. One line, present in the electron diffraction pattern, was missing in the X-ray powder diagram, which might be due to a certain orientation of the crystals in the present case.

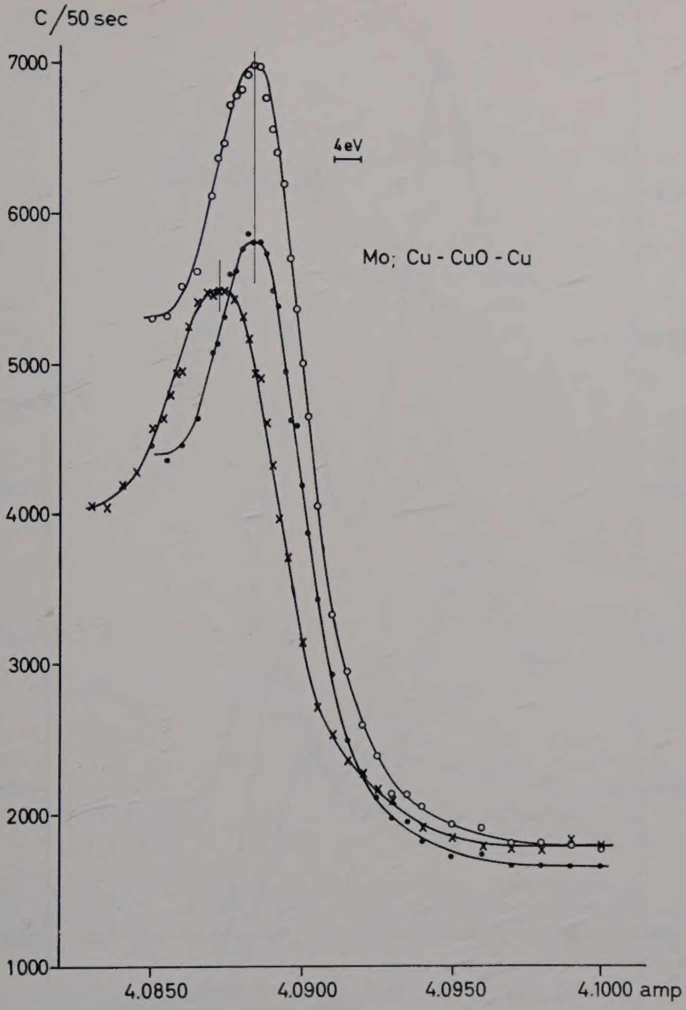

Fig. 6. CuK(Mo$K\alpha_1$) photo lines. The curves plotted with open and filled circles are the photo lines of metallic copper, which had been evaporated on the outer sections of the source holder. The photo line of the cupric oxide, which is plotted with crosses, falls at a lower spectrometer current, indicating a higher K binding energy in the oxide. It is seen that the K photo line from metallic copper falls at a different current than the same lines in Fig. 3. This is due to a different source position.

metal, indicating a greater binding energy in the oxide. From the fourteen runs made, an average shift of (4.4 ± 0.5) eV was obtained, the greatest deviation from the mean value being 1.3 eV. In the case of the K photo lines, there was no difficulty in obtaining a satisfactory intensity, the peak counting rate often being more than 5000 counts per minute, with a peak-to-background ratio better than 2.5.

L_{I} *shift.*—The conditions for determining the L_{I} level shifts were less favourable, since the conversion probability of the Mo $K\alpha_1$ radiation is considerably lower here,

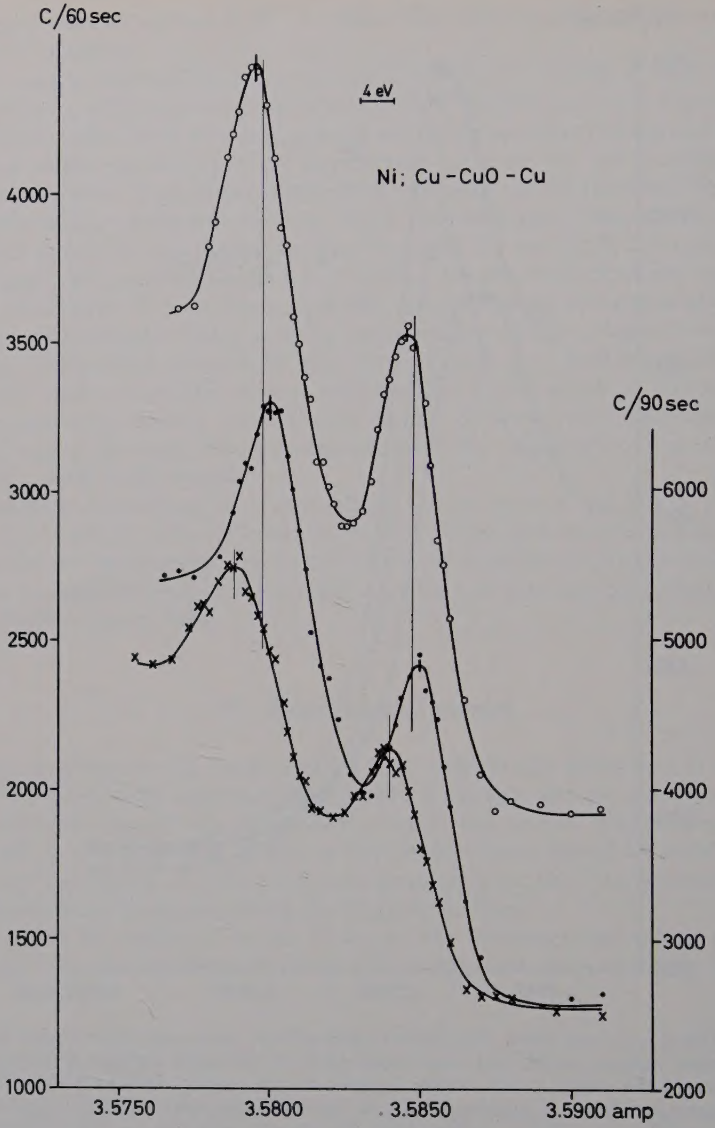

Fig. 7. L_{II} and L_{III} photo lines from metallic copper (open and filled circles, left ordinate axis) and from cupric oxide (crosses, right ordinate axis). In this case Ni $K\alpha$ radiation was used for the production of photo electrons. The interpolated position of a "zero shift" line from the middle section of the source holder is marked with a vertical line equidistant from the peaks of the photo lines from the outer sections.

and, furthermore, the CuL_I(Mo$K\alpha_1$) line falls at a higher energy than the corresponding K line. Four measurements were made, giving an average shift of (4.4 ± 1.0) eV towards greater binding energy in the oxide. The best peak intensity obtained was around 2500 cpm, with a peak-to-background ratio of 1.5.

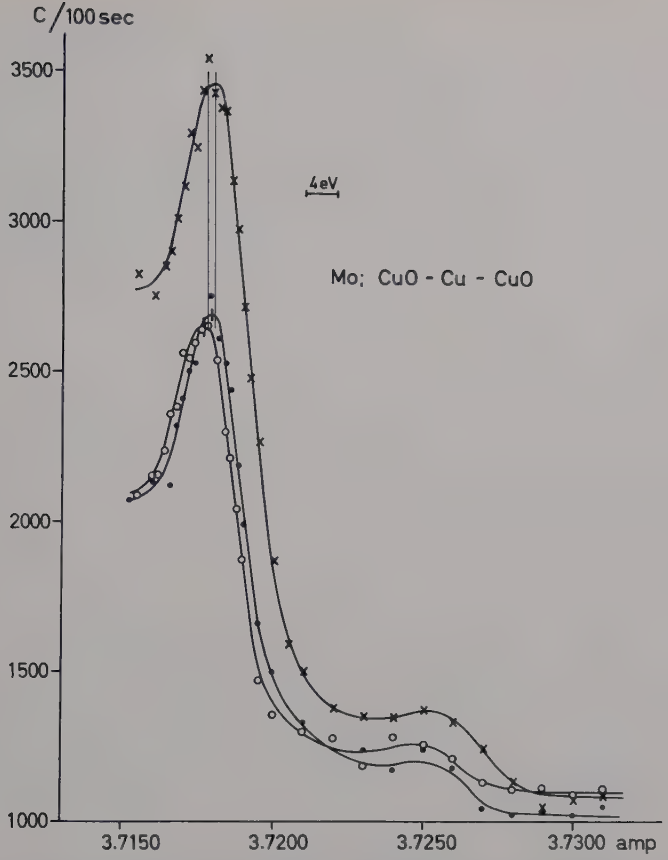

Fig. 8. The strongest Auger line in the *KLL* group (*A*6 in ref. [1]) from metallic copper (crosses) and from cupric oxide (open and filled circles). Here the shift is considerably smaller than for the photo lines. The weak line at about 3.725 amps is the *A*7 Auger line (see ref. [1]).

L_{II} and L_{III} shifts (Fig. 7).—For measurements of the L_{II} and L_{III} shifts, the $K\alpha_1$ radiation of Ni was chosen as a monochromatic energy source. This was done in order to obtain better intensity and also to bring the spectrum down to a lower energy region (6.5 keV), where it would be possible to resolve the two components. (The reason why the L_I shift was not also measured with a Ni anode was that the CuL_1(Ni $K\alpha$) lines coincide with the Cu K Auger spectrum, which is excited by the continuous X-radiation.) Of the L_{III} shifts, four measurements were made, giving an average of (2.5 ± 0.8) eV towards greater binding energy in the oxide. The best peak intensity obtained was 3500 cpm with a peak-to-background ratio of 1.8.

The position of the L_{II} photo line is difficult to determine unambiguously, since it coincides with the Cu L_{III}(Ni $K\alpha_2$) line as well as with the peak of electrons belonging to Cu L_{III}(Ni $K\alpha$)$_1$, but scattered inelastically with a discrete energy loss. Two measurements were made of the L_{II} shift, giving the average value (3.3 ± 1.5) eV.

Auger line (A6) shift (Fig. 8).—For these measurements was chosen the strongest line in the K Auger spectrum of Cu, (7033 eV), which has previously been shown to correspond to the transition $1s^1 2s^2 2p^6 \rightarrow 1s^2 2s^2 2p^4$. Several factors make this line very suited for the study of shifts: when Mo radiation is used for ionizing the K level, the intensity of the Auger line is high (at least 2000 cpm, peak-to-background ratio = 3.5). Also, the line is narrow, since the spectrometer window curve is narrow at this energy and the width of the Mo $K\alpha$ line does not enter. The average value of the shift, obtained from five measurements, is (1.0 ± 0.3) eV towards lower energy in the oxide. For heavy elements, where j-j coupling dominates, it has been found that the $KL_{II}L_{III}$ Auger line is the strongest. It can be expected that the nature of the coupling contributes only second order effects in the energy *shifts* of the Auger lines on going from the metal to the oxide. Neglecting the considerable admixture of L–S coupling in the case of Cu and identifying $A6$ with the $KL_{II}L_{III}$ transition, we obtain for the $A6$ shift

$$\Delta E(A6) = \Delta K - \Delta L_{II} - \Delta L_{III} = (-1.4 \pm 1.8)\,\mathrm{eV}$$

where we have given the r.m.s. error. This value is in good agreement with the shift of (-1.0 ± 0.3) eV obtained directly for the $A6$ Auger line.

All energy shifts are summarized in Table 1.

Table 1.

Level	Energy shift Cu→CuO (eV)	Energy shift Cu→Cu$_2$O (eV)
K	$+4.4 \pm 0.5$	$+0.7 \pm 0.8$
L_I	$+4.4 \pm 1.0$	—
L_{II}	$+3.3 \pm 1.5$	—
L_{III}	$+2.5 \pm 0.8$	—
Auger line	-1.0 ± 0.3	—

(ii) *Line widths*

The experimental width, w_{tot}, of a line is made up of two components, one being the sum of the natural widths of the levels involved, w_{nat}, and the other being the width of the spectrometer window curve, w_{sp}. We assume that these two components combine according to the formula

$$w_{\mathrm{tot}}^n = w_{\mathrm{nat}}^n + w_{\mathrm{sp}}^n, \tag{1}$$

where we have chosen the same exponent for all three terms in order to conserve dimensions. If the natural line shape and the spectrometer window curve were both of the form $1/(1+x^2)$, n would be equal to 1. If both were gaussian, n would be equal to 2. For most lines w_{nat} can be obtained from X-ray data. For the spectrometer window at different current settings we have, for unrelativistic energies, the relation

$$\frac{w_{\mathrm{sp}}(\mathrm{I}_1)}{\mathrm{I}_1} = \frac{w_{\mathrm{sp}}(\mathrm{I}_2)}{\mathrm{I}_2}. \tag{2}$$

From two measured lines, for which w_{nat} is known, we then get a system of two equations of the form (1) and one of the form (2), which we can solve for n and w_{sp} (I). These values can then in turn be employed to analyze lines, whose natural widths are not known.

Since the lines were not completely resolved from the peak due to inelastically scattered electrons, the line width was taken to be twice the half width of the high energy flank. By the method described above, using the Cu K(Mo $K\alpha_1$) and the Cu L_{III}(Ni $K\alpha_1$) photo lines, it was found that n was very close to 1 and the width of the spectrometer window curve at the Cu K(Mo $K\alpha_1$) energy was 8.2 eV. Table 2 gives the natural widths of the different lines in the metal as well as in the oxide. The widths in column I that are marked with an asterisk are deduced from X-ray data [7, 8, 9], and these values are used in the calculations of the other line widths. The errors given in the table only pertain to the present measurements, since these are the only ones that are relevant for the change in line width on going from the metal to the oxide.

Table 2.

Line	I w_{nat} (eV) Cu	II w_{nat} (eV) CuO	II − I (eV)	II − I (% of I)
Cu K(Mo $K\alpha_1$)	7.4*	8.6 ± 0.5	1.2 ± 0.7	16 ± 9
Cu L_{I} (Mo $K\alpha_1$)	8.0 ± 1.0	> 8.0	> 0	> 0
Cu L_{III} (Ni $K\alpha_1$)	2.8*	3.1 ± 0.8	0.3 ± 1.1	10 ± 40
A6	4.4 ± 0.3	3.4 ± 0.3	-1.0 ± 0.4	-23 ± 9

B. *Cu—Cu$_2$O*

Shift of K binding energy.—Two measurements were made of the energy shift of the Cu K(Mo $K\alpha_1$) line on going from metallic copper to the cuprous oxide, giving an average value of (0.7 ± 0.8) eV.

V. Discussion

A. *Energy shifts*

The interpretation of the results is complicated by the fact that different types of solids are represented in this investigation: a metal (Cu) and two semiconductors (Cu_2O and CuO). The electron diffraction patterns show that although the samples were prepared in very thin layers, the crystallization was the normal one. In Cu_2O, the semiconductor properties at room temperature are ascribed to oxygen impurities, whereas CuO is thought to be an intrinsic semiconductor. These interpretations are supported by experimental results concerning the electronic conductivity of the two oxides [10, 11]. For exact stoichiometric compositions of the oxides at 20°C, the conductivity for CuO is reported to be 6.4×10^{-4} ohm^{-1}cm^{-1} and that of Cu_2O,

3×10^{-9} ohm^{-1}cm^{-1}. For the cuprous oxide the conductivity is sensitive to the partial oxygen pressure of the surrounding medium, whereas for cupric oxide no such correlation has been observed.

We shall give a brief discussion of the different types of solids in terms of their band structure and compare the present results with those obtained by conventional X-ray methods. Fig. 9 is a schematic energy level diagram of a metal and an intrinsic semiconductor. It is well known [12] that the Fermi level energy for an insulator or an intrinsic semiconductor may be written as

$$E_F = \tfrac{1}{2}(E_c + E_v) + \tfrac{3}{4}kT \ln \frac{m_h^*}{m_e^*}, \tag{3}$$

under the usual assumptions of low concentration of carriers and quadratic dependence on momentum in the upper and lower parts of the valence and conduction bands respectively. Here E_c and E_v are the bottom energy of the conduction band and the top energy of the valence band, respectively; m_e^* is the effective mass of an electron in the conduction band and m_h^* that of a hole in the valence band. Since the last term usually does not exceed 0.1 eV at room temperature and thus can be neglected for our purposes, the Fermi level can be treated as being halfway between the valence and the conduction band.

Let us now consider the X-ray absorption spectrum of an insulator or intrinsic semiconductor. If the K absorption edge is simple, we can find a certain point on it that represents the transition of a K electron into the lowest part of the conduction band. Similarly we can, in principle, find a point on the X-ray emission curve that corresponds to a transition from the highest part of the valence band down to the K level. In simple absorption and emission spectra these points are usually identified with the first points of inflection. In view of Fig. 9 it is to be expected that, for a pure metal, the points of inflection of the emission and absorption curves should coincide, since in this case they both correspond to the Fermi level. This has also been found to be the case e.g. for metallic Al [13]. As the solid is transformed into an insulator or intrinsic semiconductor, e.g. by oxidation, one must expect the points of inflection to move apart: that of the absorption curve towards higher energy with respect to that of the emission curve. According to our approximation, the Fermi level is located halfway between the two points and we can thus determine whether the K level (origin in Fig. 9) has shifted with respect to the Fermi level: if this is the case, the points of inflection will shift asymmetrically with respect to their original position in the pure metal. The shift of the K level with respect to the Fermi level is given by

$$\Delta E_{K-F} = \tfrac{1}{2}(\Delta E_c + \Delta E_v), \tag{4}$$

where ΔE_c and ΔE_v are the shifts of the absorption and emission curves.

It is clear that the conventional X-ray method for determining level shifts depends strongly on the correct interpretation of the structure of absorption and emission spectra, which, in many cases, is a serious draw-back. In order to apply the above reasoning, it may for instance be necessary to know the detailed nature of the electronic states in the conduction and valence bands. These problems do not arise in the present investigation. However, one difficulty lies in the fact that, whereas in X-ray studies one is only concerned with level *spacings*, we must, in the present

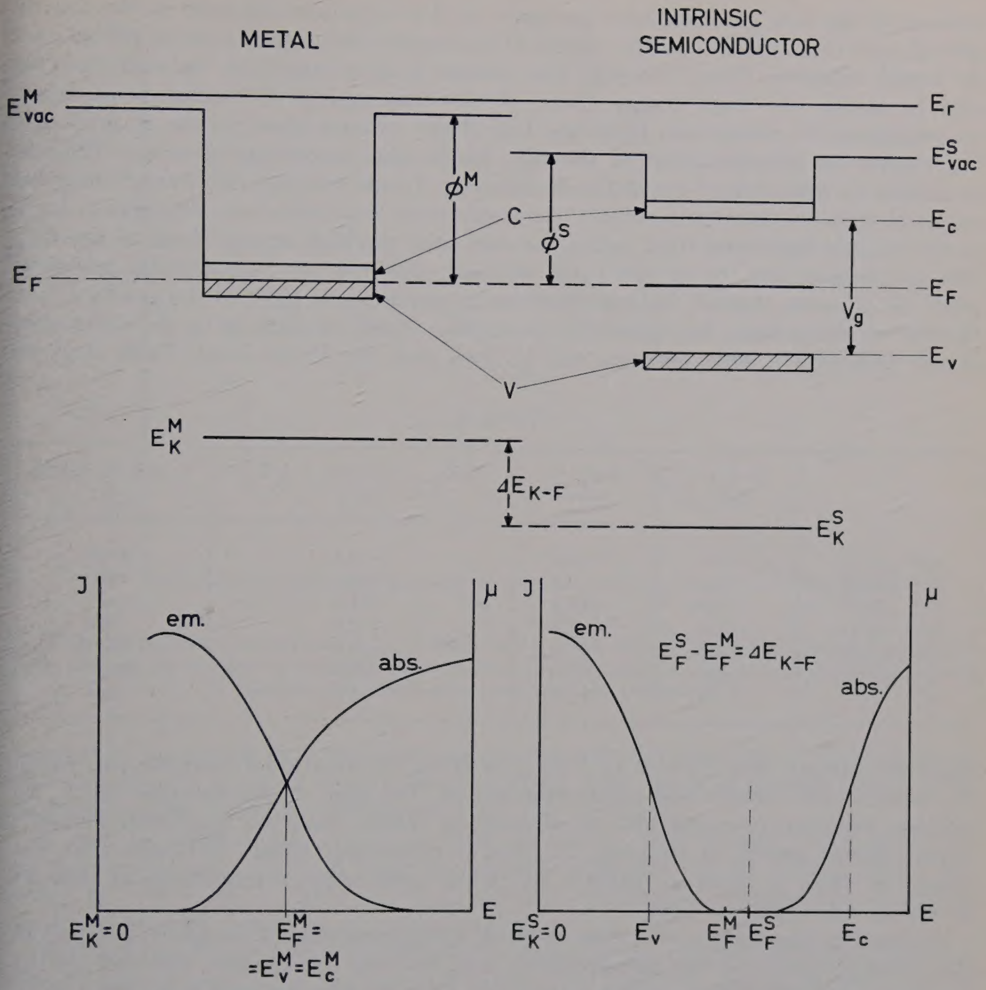

Fig. 9. The upper part of the figure shows schematic energy diagrams of a metal and an intrinsic semiconductor. E_r = reference potential outside source; E_{vac} = vacuum level; E_c = bottom of conduction band; E_v = top of valence band; $E_K = K$ level; C = conduction band; V = valence band; ϕ = work function. Below the energy diagrams are given schematic illustrations of X-ray absorption and emission curves for the metal and the semiconductor, respectively.

case, compare actual energy levels. As our reference level we chose the Fermi level of the pure metal. It is a well-known fact that for two crystals in contact the equilibrium condition is that the Fermi levels coincide. For metals, this equilibrium condition is reached instantaneously, and also for semiconductors the time that elapses before equilibrium is established is negligible for our purposes. Since the sample is always grounded, the Fermi level is fixed in all three cases (metallic copper, CuO and Cu_2O), and the chemical shifts that are measured with respect to a reference potential outside the source (E_r) are equivalent to the shifts relative to the Fermi levels.

Sanner, in his thesis [14], reports the energies of the X-ray K absorption edges as well as of the $K\beta_5$ emission lines for some of the transition elements in the fourth period and their oxides. In the metals of this period the upper levels of the $3d$ and $4s$ bands coincide. Since the $K\beta_5$ line results from a transition between the $3d$ and $1s$ states, the high energy flank of this line may, in the metal, be assumed to correspond to transitions from the top of the valence band to the K level. In the oxides the interpretation of the $K\beta_5$ line is more uncertain, since it is difficult to predict to what extent the different electronic bands overlap. However, it may be assumed that the admixture of oxygen states with large quantum numbers is high in the valence band and that, again, we may take the high energy flank of the $K\beta_5$ line to represent the top of this band, without violating any fundamental selection rules. In all cases studied, Sanner obtained an asymmetric shift of the points of inflection on going from the metals to the oxides, which, according to the discussion above, indicates a shift between the K level and the Fermi level. Table 3 gives Sanner's primary data as well as ΔE_{K-F} as given by equation 4, and the gap width V_g between the valence and conduction bands. The high values obtained for V_g all indicate insulator properties for the oxides. Cu differs from the transition elements of the fourth period in that the $3d$ band is completely filled. It is seen that the values of ΔE_{K-F} given in Table 3 are of the same order of magnitude as that reported in this work for CuO.

Table 3.

	ΔE_v (1) (eV)	ΔE_c (1) (eV)	$\Delta E_{K-F} = \frac{1}{2}(\Delta E_c + \Delta E_v)$ (eV)	$V_g = \Delta E_c - \Delta E_v$ (eV)
$Ni^0 \to N^{+3}$	−1.1	+9.9	+4.4	11.0
$Co^0 \to Co^{+3}$	−2.4	+9.7	+3.7	12.1
$Fe^0 \to Fe^{+3}$	−2.5	+12.1	+4.8	14.6
$Mn^0 \to Mn^{+2}$	−1.4	+5.4	+2.0	6.8
$Cr^0 \to Cr^{+3}$	−4.6	+10.4	+2.9	15.0
$V^0 \to V^{+5}$	−3.1	+17.0	+7.0	20.1
$Ti^0 \to Ti^{+4}$	−1.6	+12.3	+5.4	13.9

Sanner has also measured a shift in the K absorption edge of copper on going from the metal to CuO, but the corresponding $K\beta_5$ line was not studied. For ΔE_c in the reaction Cu → CuO Sanner reports the value +4.7 eV, which would require a $\Delta E_v = +4.1$ eV in order to be compatible with the present result that $\Delta E_{K-F} = 4.4$ eV. This would give a gap width of 0.6 eV between the conduction band and the valence band, which is a typical value for an intrinsic semiconductor. The gap width of an intrinsic semiconductor is related to the electronic conductivity, σ, by the following expression [15]:

$$\sigma = 2\,|e|\,(2\pi k T/h^2)^{\frac{3}{2}}\,(m_e^* m_h^*)^{\frac{3}{4}}\,e^{-V_g/2kT}\,(\mu_e + \mu_h), \qquad (5)$$

where again m_e^* and m_h^* are the effective masses of electrons and holes and μ_e and μ_h are the mobilities. Since the temperature dependence is dominated by the exponential factor, the gap width can be obtained from the slope of ln σ as a function of $1/T$. Those quantities are plotted for CuO in Fig. 10, where the conductivity data are taken from LeBlanc *et al.* [10]. From the curve we obtain for the gap width the

---

[1] Taken directly from table 62 of reference [14].

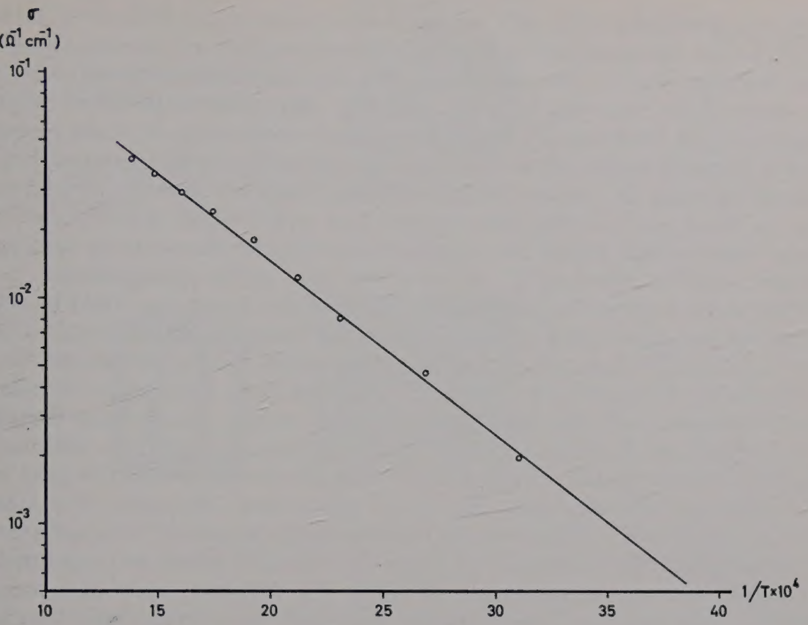

Fig. 10. Conductivity (as measured by LeBlanc and Sachse, ref. [10]) of CuO, plotted logarithmically against the inverse of the absolute temperature. The slope of the line gives the separation between the conduction band and the valence band.

value 0.31 eV, which is in very good agreement with the value 0.6 eV obtained from the data of the present investigation together with those of Sanner, considering that differences between energies of 8 keV are involved.

It may be pointed out that the shift of the Cu $K\alpha_1$ line on going from the metal to the cupric oxide, deduced from the present values for the K and L_{III} photo line shifts, is $+1.9 \pm 1.3$ eV. This is in disagreement with Sanner's conclusions, according to which no shift should be expected for CuO.

For Cu_2O no X-ray data are available. It would at any rate be impossible to make direct comparisons, since the cuprous oxide is an impurity semiconductor, and it would be difficult to locate the Fermi level with the aid of absorption and emission curves.

B. *Line widths*

In the cases of the photo lines there is an indication of line broadening on going from the metal to the oxide. Before ascribing any physical significance to this fact, one must consider the possibility that, during the heating of the oxide sample, some surface diffusion might have taken place, spreading the copper over a greater part of the backing. However, no such spread could be detected visually; also, no broadening of the K photo line was observed, when the source had been heated in a hydrogen atmosphere. Finally, we have the result that the most drastic change in line width, in the case of the Auger line ($A6$), was in the opposite sense: the width was found to *decrease* by 23 % on oxidation.

As shown in reference [1], the $A6$ line corresponds to the transition $1s^1 2s^2 2p^6 \rightarrow 1s^2 2s^2 2p^4$. In the case of copper, where the electronic coupling is intermediate between Russell–Saunders and j-j, we can expect five lines in this transition, corresponding to the final states ${}^1S_0$, ${}^1D_2$, ${}^3P_0$, ${}^3P_1$, and ${}^3P_2$. The relative positions of the lines were calculated in reference [1]. Considering these calculations, it might be suspected that $A6$ is actually composed of several lines, primarily those corresponding to the final states ${}^3P_1$ and ${}^3P_0$, whose theoretical separation is 4.5 eV in metallic copper. In view of the fact that the total natural line width of $A6$ is only 4.4 eV, we can no longer assume this line to be complex, if we consider the coupling and screening parameters, used in reference [1], to be of the right order of magnitude.

In order to see whether the decrease in width of the Auger line could be related to a decrease of the Auger yield with oxidation, the intensity ratio between the Auger line and the Cu K(Mo $K\alpha_1$) photo line was determined for the metal and the cupric oxide. Since the lines are not completely resolved from the peaks of inelastically scattered electrons, only the surfaces of the high energy halves were measured. It must be pointed out that the measured intensity ratios do not give the absolute K Auger yield, since ionization of the K shell occurs from interaction not only with the Mo $K\alpha$ radiation but also with the X-ray continuum. Measuring the Auger lines against the Cu K(Mo $K\alpha_1$) lines merely normalizes the intensity to equal amounts of converter material. Since each pair of Auger-Cu K(Mo $K\alpha_1$) lines was measured within a short time interval, the procedure of taking the intensity ratio also corrects for longtime variations of the X-ray intensity. For CuO, the average ratio was found to be 0.87, and for metallic Cu, 1.16. Hence, the K Auger intensity for CuO is 25 % lower than for Cu. This is in agreement with the result that the line width decreases by 23 % on oxidation. It might be mentioned in this connection that Nordfors [16], on studying the $K\alpha_3$ and $K\alpha_4$ X-ray satellites of Al and Al_2O_3 (corresponding to transitions from an initial state with singly ionized K and L shells to a final state with a doubly ionized L shell), found intensity variations on going from the metal to the oxide, which might also be attributed to changes in the transition probabilities.

Institute of Physics, University of Uppsala.

REFERENCES

1. Sokolowski, E., Nordling, C., and Siegbahn, K., Arkiv f. Fysik *12*, 301 (1957).
2. Siegbahn, K., and Edvarson, K., Nuc. Phys. *1*, 137 (1956).
3. Gulbransen, E. A., and McMillan, W. R., Journal Electrochem. Soc. *99*, 393 (1952).
4. Dunholter, H., and Kersten, H., Journal Appl. Phys. *10*, 523 (1939).
5. White, A., and Germer, L., Trans. Electroch. Soc. *81*, 305 (1942).
6. Allen, J. A., Trans. Faraday Soc. *48*, 273 (1952).
7. Brogren, G., Phys. Rev. *96*, 589 (1954).
8. Bearden, J. A., and Shaw, C. H., Phys. Rev. *48*, 18 (1935).
9. Sørum, H., Kongl. Norske Vidensk. Selskab. *19*, 44 (1946).
10. Le Blanc, M., and Sachse, H., Ann. Phys. *11*, 727 (1931).
11. v. Baumbach, H. H., Dunwald, H., and Wagner, C., Zeitschr. Phys. Chem. *22*, 227 (1931).
12. Dekker, A. J., Solid State Physics. Prentice-Hall, Inc. (1957), p. 309.
13. Rudström, L., Arkiv f. Fysik *12*, 287 (1957).
14. Sanner, V. H., Thesis, Uppsala (1941).
15. Kittel, C., Introduction to Solid State Physics. John Wiley & Sons, Inc. (1956), p. 351.
16. Nordfors, B., Arkiv f. Fysik *10*, 279 (1956).

Tryckt den 23 april 1958

Uppsala 1958. Almqvist & Wiksells Boktryckeri AB